THE JOURNAL OF BIOLOGICAL CHEMISTRY
Vol. 278, No. 29, Issue of July 18, pp. 26356–26364, 2003

Printed in U.S.A.

The C Terminus (Amino Acids 75–94) and the Linker Region (Amino Acids 42–54) of the Ca^{2+}-binding Protein S100A1 Differentially Enhance Sarcoplasmic Ca^{2+} Release in Murine Skinned Skeletal Muscle Fibers*

Received for publication, April 1, 2003, and in revised form, April 23, 2003
Published, JBC Papers in Press, April 28, 2003, DOI 10.1074/jbc.M303338200

Patrick Most‡, Andrew Remppis‡, Cornelia Weber§, Juliane Bernotat¶, Philipp Ehlermann, Sven T. Pleger¶, Wolfgang Kirsch§, Martin Weber§, Dietmar Uttenweiler§, Godfrey L. Smith‖, Hugo A. Katus, and Rainer H. A. Fink§**‡‡**

From the Abteilung Innere Medizin III (Kardiologie), Universität Heidelberg, 69115 Heidelberg, Germany, §Institut für Physiologie und Pathophysiologie, Medizinische Biophysik, Im Neuenheimer Feld 326, Universität Heidelberg, 69120 Heidelberg, Germany, and ‖Institute of Biomedical Life Science, University of Glasgow, G128QQ Glasgow, United Kingdom

S100A1, a Ca^{2+}-binding protein of the EF-hand type, is most highly expressed in striated muscle and has previously been shown to interact with the skeletal muscle sarcoplasmic reticulum (SR) Ca^{2+} release channel/ryanodine receptor (RyR1) isoform. However, it was unclear whether S100A1/RyR1 interaction could modulate SR Ca^{2+} handling and contractile properties in skeletal muscle fibers. Since S100A1 protein is differentially expressed in fast- and slow-twitch skeletal muscle, we used saponin-skinned murine *Musculus extensor digitorum longus* (EDL) and *Musculus soleus* (Soleus) fibers to assess the impact of S100A1 protein on SR Ca^{2+} release and isometric twitch force in functionally intact permeabilized muscle fibers. S100A1 equally enhanced caffeine-induced SR Ca^{2+} release and Ca^{2+}-induced isometric force transients in both muscle preparations in a dose-dependent manner. Introducing a synthetic S100A1 peptide model (devoid of EF-hand Ca^{2+}-binding sites) allowed identification of the S100A1 C terminus (amino acids 75–94) and hinge region (amino acids 42–54) to differentially enhance SR Ca^{2+} release with a nearly 3-fold higher activity of the C terminus. These effects were exclusively based on enhanced SR Ca^{2+} release as S100A1 influenced neither SR Ca^{2+} uptake nor myofilament Ca^{2+} sensitivity/cooperativity in our experimental setting. In conclusion, our study shows for the first time that S100A1 augments contractile performance both of fast- and slow-twitch skeletal muscle fibers based on enhanced SR Ca^{2+} efflux at least mediated by the C terminus of S100A1 protein. Thus, our data suggest that S100A1 may serve as an endogenous enhancer of SR Ca^{2+} release and might therefore be of physiological relevance in the process of excitation-contraction coupling in skeletal muscle.

S100A1, a low molecular mass (M_r 10,000) Ca^{2+}-binding protein of the EF-hand type, belongs to the multigenic S100 protein family whose members have been implicated in the Ca^{2+}-dependent regulation of a variety of cellular functions including Ca^{2+} homeostasis and contractility of striated and smooth muscle tissue (1–3). S100 proteins form an important subclass of EF-hand proteins that are typically small, ~90 residues (two EF-hand modules), and dimeric. These proteins, evolutionary highly conserved, display a tissue- and cell-specific expression pattern, a characteristic they share with most other EF-hand Ca^{2+}-binding proteins (*e.g.* troponin) but not with the multifunctional and ubiquitously expressed calmodulin (for review see Ref. 4). S100A1 is the most abundant S100 protein in striated muscle and has been shown to colocalize, in particular, with structures involved in excitation-contraction coupling in skeletal as well as cardiac muscle (5–7).

Although subsequent physiological studies in cardiac muscle recently identified S100A1 as a novel regulator of cardiac contractility being essential for cardiac reserve (8–11), significantly less is known regarding the impact of S100A1 on contractile properties of skeletal muscle. Biochemical and biophysical studies, however, have indicated that S100A1 can physically interact with the purified sarcoplasmic Ca^{2+} release channel/ryanodine receptor skeletal muscle isoform (RyR1)[1] (12), the molecular entity that is the key substrate for sarcoplasmic reticulum (SR) Ca^{2+} release in striated muscle. However, it was unclear whether S100A1/RyR1 interaction is able to enhance Ca^{2+} release from the intact SR to increase contractile performance in skeletal muscle fibers. We therefore sought to investigate the role of S100A1 protein in saponin-skinned slow-twitch (*Musculus soleus*, Soleus) and fast-twitch (*Musculus extensor digitorum longus*, EDL) murine skeletal muscle fibers maintaining structural and functional integrity of the SR and the contractile apparatus. This approach enabled

* This work was supported in part by Bundesministerium für Bildung und Forschung Grant I3N7871 and Deutsche Forschungsgemeinschaft Grant 240/3–1 (to R. F. and D. U.), the British Heart Foundation (to G. S.), the Forschungsförderung Medizinische Fakultät der Universität Heidelberg Grants 93/2002 and 61/2003 (to P. M.), and the Deutsche Forschungsgemeinschaft Grant Re1083/1-1 (to A. R.). The costs of publication of this article were defrayed in part by the payment of page charges. This article must therefore be hereby marked "*advertisement*" in accordance with 18 U.S.C. Section 1734 solely to indicate this fact.

‡ These authors contributed equally to this work.
¶ Supported by the Boehringer Ingelheim Stiftung.
** These authors contributed and supported this work equally.
‡‡ To whom correspondence should be addressed: Institut für Physiologie und Pathophysiologie, Im Neuenheimer Feld 326, Universität Heidelberg, 69120 Heidelberg, Germany. Tel.: 49-6221-54-4065; Fax: 49-6221-54-4123; E-mail: rainer.fink@agfink.de.

[1] The abbreviations used are: RyR, release channel/ryanodine receptor; skeletal muscle isoform; SR, sarcoplasmic reticulum; Soleus, *M. soleus*; EDL, *M. extensor digitorum longus*; aa, amino acid; ANOVA, analysis of variance; N, N-terminal; H, hinge region; C, C-terminal; pCa, $-\log[Ca^{2+}](M)$; SERCA, SR Ca^{2+}-ATPase.

us to assess the effect of S100A1 on SR Ca^{2+} release and the interplay between preserved SR and contractile apparatus function (13).

In general, S100 proteins consist of an N-terminal part containing a non-conventional Ca^{2+}-binding site of the EF-hand (helix-loop-helix) type and a C-terminal part containing a canonical EF-hand. The two parts are interconnected by an intermediate region, the "hinge region," and the C-terminal EF-hand is followed by a C-terminal extension. The hydrophobic hinge region and the C-terminal extension display the least amount of sequence identity among S100A1 members and are suggested to specify the biological activities of individual S100A1 proteins. S100 proteins typically display structural changes and exposure of hydrophobic surfaces upon Ca^{2+} binding, reminiscent of the sensor properties of calmodulin, to interact with their target proteins. Based on novel insights gathered from structural analysis of S100A1 protein (14), a S100A1 peptide model consisting of the region amino acids 2–16 (Fig. 1*C*, *N-terminal* (*N*)), amino acids 42–54 (*Hinge-region* (*H*)), and amino acids 75–94 (*C-terminal* (*C*)) devoid of Ca^{2+}-binding motifs was synthesized to gain further insight into structure-function relationship of S100A1/RyR1 interaction as well as to exclude adverse Ca^{2+}-buffering effects by the native protein (15, 16)

Taking advantage of chemically skinned skeletal muscle fibers, we were able to demonstrate for the first time that S100A1/RyR1 interaction can enhance SR Ca^{2+} release from the intact SR resulting in increased isometric force transients both in slow- and fast-twitch skeletal muscle. Importantly, S100A1 protein as well as the synthetic S100A1 peptide model (N/H/C) equally enhanced functional parameters, and these effects were found to be dose-dependent in a range of 0.001–10 μM. Further testing of single S100A1 domains identified the hydrophobic C-terminal extension (aa 75–94) as well as the hinge region (aa 42–54) to differentially affect SR function. These effects are apparently based on enhanced SR Ca^{2+} release as S100A1 neither influenced SR Ca^{2+} uptake nor myofilament Ca^{2+} sensitivity/cooperativity in skeletal muscle fibers in our experimental setting. Thus, our data suggest a putative physiological role for S100A1 to serve as an endogenous enhancer of SR Ca^{2+} release in skeletal muscle.

EXPERIMENTAL PROCEDURES

Production of Recombinant Human S100A1 Protein and Synthetic Peptides—Recombinant human S100A1 protein was expressed and purified as previously described (17), whereas purity and relative mass of S100A1 protein preparations were confirmed as described earlier (1, 10). S100A1 peptides (N-terminal (S100A1-N), aa 2–16; hinge region (S100A1-H), aa 42–54; C-terminal (S100A1-C), aa 75–94; human S100A1, Swiss Protein Data Base number P23297 (18)) were generated custom-based by the use of continuous flow N-terminal Fmoc (*N*-(9-fluorenyl)methoxycarbonyl) group-protected solid-phase peptide synthesis (Eurogentec, Seraing, Belgium). Purity was analyzed by SDS-PAGE and analytical reverse-phase high performance liquid chromatography as described previously (1) while accurate molecular mass was obtained by matrix-assisted laser desorption ionization-time of flight mass spectroscopy (19). Silver staining of polyacrylamide gels was performed according to Oakley *et al.* (20). Both S100A1 protein and peptides were dialyzed against 10 mM HEPES, pH 7.4, and stored in aliquots at −80 °C.

Muscle Fiber Preparation and Experimental Solutions—All of the animals were handled according to the guidelines of the animal care committee of the University of Heidelberg. Male BALB/c mice (3–6-months-old) were sacrificed by an overdose of carbon dioxide, and muscle fiber preparation was carried out as previously described (21, 22). Either EDL or Soleus was isolated, and a small fiber bundle containing two to four single fibers (between 80 and 150 μm in diameter and 3–4-mm-long) was dissected in paraffin oil. The fiber preparation was glued between a force transducer pin (AE801, Senso-Noras, Horton, Norway) and a micrometer-adjustable screw. All of the experiments were carried out at room temperature (23–25 °C). All of the solutions were adjusted to pH 7.0. The free ion concentrations were calculated with the computer program REACT (version 2.0) from G. L. Smith (Glasgow, Scotland). Table I shows the concentrations of the solution used in the experiments. The high relaxation and the high activation solution contained 50 mM EGTA to buffer free Ca^{2+}, whereas the low relaxing solution contained 0.5 mM EGTA and 49.5 mM 1,6-diamino hexane-*N*,*N*,*N*,*N*-tetraacetic acid (HDTA), which in contrast to EGTA has very low affinity to Ca^{2+}. The skinning solution is obtained by the addition of 50 μg/ml saponin to the low relaxing solution. The release solution consisted of the low relaxing solution with 5 mM caffeine added. Loading solution contained 50 mM EGTA to clamp free Ca^{2+} to 0.4 μM (pCa 6.4). The solutions to measure the pCa-force relation were obtained by mixing high relaxing solution with appropriate amounts of high activating solution, and 5 mM caffeine added. All of the experiments were recorded using a strip chart recorder and were simultaneously digitally converted with an Axon Instruments Digidata 1200 board and interface (using the Axotape Software, version 2.0) and stored on the computer (22).

TABLE I
Total concentration, in brackets is free concentration
LR, low relaxing solution; HR, high relaxing solution; HA, high activation solution; SK, skinning solution; LS, loading solution.

	LR	HR	HA	SK	LS
ATP (mM)	8	8	8	8	8
CP (mM)	10	10	10	10	10
CK (unit/ml)	150	150	150	150	150
Ca^{2+} (mM)		0.01	49.5		$[4 \times 10^{-4}]$
Mg^{2+} (mM)	[0.5]	[0.5]	[0.5]	[0.5]	[0.5]
Na^{+} (mM)	36	36	36	36	36
K^{+} (mM)	117	117	117	117	117
HEPES (mM)	60	60	60	60	60
EGTA (mM)	0.5	50	50	0.5	50
HDTA (mM)	49.5			49.5	
Saponin (mg/ml)				50	

Assessment of Ca^{2+}-induced Isometric Twitch Force and Ca^{2+} Transients—Muscle fibers were skinned for 5 min in skinning solution while the sarcomere length was adjusted to 2.6 ± 0.1 μm using the diffraction pattern of a helium-neon laser (22). Before loading the SR with the loading solution (pCa 6.4) for 1 min, the fibers were shortly immersed in release solution and high relaxing solution and then equilibrated for 2 min in low relaxing solution. Subsequently, the preparation was dipped for 1 s into the high relaxing solution and again for 2 min in low relaxing solution. The fibers were exposed to the release solution containing 5 mM caffeine until the initial force transient returned to the resting force level. Maximum force was measured in the high activating solution at pCa 4.28 and 5 mM caffeine. The fibers then were relaxed in high relaxing solution for 1 min to buffer Ca^{2+}. Several control transients were recorded before the fiber was exposed to S100A1, and the experiment was repeated as outlined above. S100A1 protein or peptides were added to the low relaxing solution before and during release and to the high activating solution (22). The pCa-force relation in response to S100A1 interventions (0.001–10 μM) was measured with six different Ca^{2+} concentrations (EDL, pCa 9.07, 5.91, 5.72, 5.49, 5.17, and 4.28; Soleus, pCa 9.07, 5.72, 5.49, 5.35, 5.17, and 4.28), each containing 5 mM caffeine. The EC_{50} and the Hill coefficient were obtained from a Hill-type fit (23). The EC_{50} value indicates the Ca^{2+} concentration needed for half-maximal isometric force activation, which is as a measure of Ca^{2+} sensitivity of the contractile apparatus. The Hill coefficient gives an indication of the maximum steepness of the sigmoidal curve. The correlation coefficients were calculated to determine the accuracy of the fit. The force transient was transformed into the corresponding free Ca^{2+} transient by using the individual pCa^{2+} force relation as a Ca^{2+} indicator and reversing each point of the force transients into the corresponding free Ca^{2+} level as previously described (22, 24, 25). Based on the fact that sensitivity of the Ca^{2+}-regulatory proteins and the corresponding force development directly provide a measure of the free myofibrillar Ca^{2+}, the pCa force relation relates free Ca^{2+} and force. Thus, the pCa-force relation can be used as a bioassay, which converts the rather slow force transients from the Ca^{2+} release from the SR into apparent Ca^{2+} transients (22, 24, 25).

Sarcoplasmic Ca^{2+} Uptake in EDL SR Vesicles—EDL muscles from hind legs of male Balb/c mice (3–6 months) were dissected and used for SR vesicle preparation as previously published (26). SR vesicle protein content was measured using the DM™ protein assay (Bio-Rad), and aliquots were stored at −80 °C. Sarcoplasmic Ca^{2+} uptake was meas-

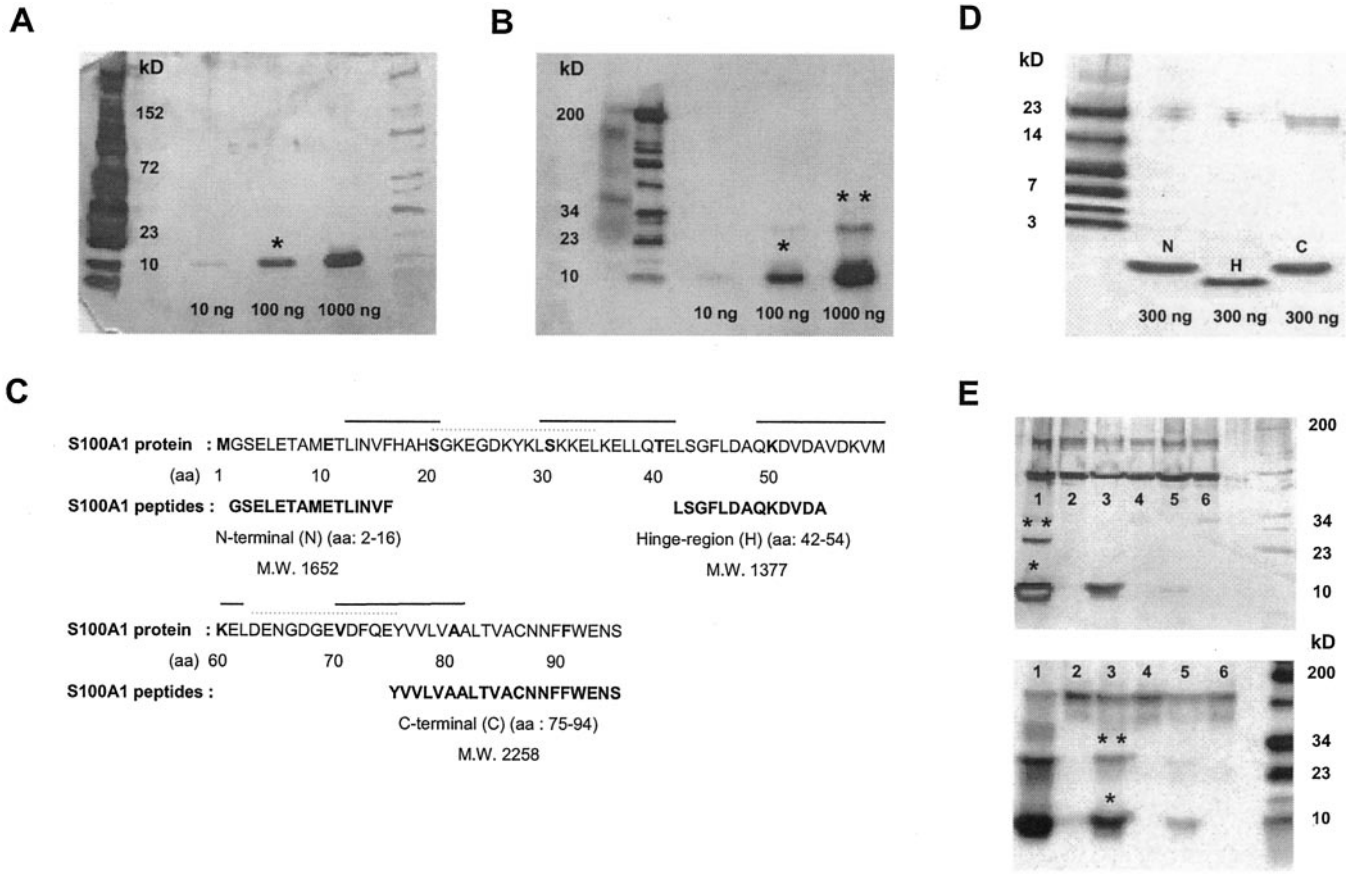

FIG. 1. **Characterization of human recombinant S100A1 protein and synthetic S100A1 peptides.** *A*, purity of human recombinant S100A1 protein was visualized by representative silver staining of increasing amounts of S100A1 protein preparations (10–1000 ng) resolved by SDS-PAGE 4–20%. S100A1 protein is indicated by *single asterisk*. *Left*, molecular masses are indicated as kDa. *B*, representative Western blot detection of S100A1 protein preparations (10–1000 ng) confirming specificity of purified S100A1 protein. S100A1 monomer and dimer are indicated by *single* and *double asterisks*, respectively. *Left*, molecular masses are indicated as kDa. *C*, amino acid sequence alignment of human S100A1 protein (aa 1–93) and selected S100A1 peptides (N/H/C). Human S100A1 protein sequence was obtained from the Swiss Protein sequence data base (18). Positions of both predicted EF-hand Ca^{2+}-binding loops are indicated by *dashed lines*, whereas s*olid bars* correspond to predicted helical elements (14). S100A1 peptide sequences (N/H/C) are shown in *boldface*, whereas aa residues and corresponding calculated molecular masses (*M.W.*) are given below. *D*, representative silver-stained SDS-PAGE 4–20% analysis of S100A1 peptides (N/H/C), indicating the high purity of the synthetic S100A1 protein domains. *Left*, molecular masses are indicated as kDa. *E*, silver staining (*upper panel*) and Western blot (*lower panel*) analysis of immunoprecipitated S100A1 protein in native and saponin-treated (*S*) murine myocardial (*heart*) and skeletal muscle (EDL and Soleus) samples. *Lane 1*, heart; *lane 2*, heart/S; *lane 3*, Soleus; *lane 4*, Soleus/S; *lane 5*, EDL; *lane 6*, EDL/S. *Right*, molecular masses are indicated as kDa.

ured as described elsewhere (27). EDL SR vesicles (100 μg) were suspended in a 1.5-ml reaction solution (in mM: 120 KCl, 5 MgATP, 15 CrP, 1 MgCl, 25 HEPES, 20 K_2Oxalate, 0.05 K_2EGTA, pH 7.0) and equilibrated with 0.01 mM Fura-2 (Sigma) and 5 μM ruthenium while stirring in a cuvette (1.5 ml). Ca^{2+} uptake measurements were started after the addition of 67 μM $CaCl_2$, resulting in an increase in free [Ca^{2+}] from ~100 nM to 1μM. The consequent decline of Fura-2 fluorescence ratio (340:380 nm) was a reflection of SR Ca^{2+} uptake, and the fluorescence ratio was recorded at 30 Hz using a spinning wheel spectrophotometer (Cairn Research). The low pass filtered (−3 db at 30 Hz) signal was digitized and stored for later analysis. Ca^{2+} uptake rate (dCa^{2+}/dt; pmol Ca^{2+}/s) for 100 μg of SR protein was obtained from the time constant (τ) of extrasarcoplasmic [Ca^{2+}] decline. τ was achieved from best-fit single-exponential decay from experiments where free $[Ca^{2+}]_i$ in the cuvette is exceeding 1 μM. The relationship between given Ca^{2+} concentrations and the resulting fluorescence ratios was established with a series of calibration experiments and analyzed according to Grynkiewicz *et al.* (28). Ca^{2+}-binding constants were taken from Fabiato and Fabiato (29) and Baudier *et al.* (15, 16). For S100A1 interventions, SR vesicles were preincubated with either 1 or 10 μM S100A1 protein or peptides (N/H/C) for 30 min while S100A1 storage buffer served as control.

S100A1 Immunoprecipitations—S100A1 protein levels in murine heart, EDL, and Soleus were assessed as previously described (30). Either untreated or saponin-skinned cardiac myocytes EDL and Soleus fibers were homogenized at 4 °C in 3 w/v phosphate-buffered saline with 5 mM EGTA/EDTA and protease inhibitor mixture (1836170, Complete Mini EDTA free, Roche Diagnostics) followed by centrifugation (10,000 × *g* for 15 min). The suspensions were rotated with bovine serum albumin-treated A/G-Sepharose for 30 min and centrifuged (800 × *g*) to remove proteins bound nonspecifically to A/G-Sepharose. The supernatants were then mixed with A/G-Sepharose and precipitating antibody for S100A1 (SA 5632) and incubated overnight at 4 °C. The samples were rotated for 30 min and centrifuged (800 × *g*), and pellets were washed three times with a buffer composed of 20 mM HEPES, pH 7.5, 150 mM NaCl, 1 mM EDTA, and 0.5% Tween 20. Samples were subjected to SDS-PAGE (4–20%), transferred to PVDF membrane, and probed with affinity-purified polyclonal S100A1-Ab (DAKO A5109). Blots were developed with the Avidix chemiluminescence detection system (Tropix, Applied Biosystems, Foster City, CA) and quantified by densitometry.

Statistical Analyses—Data are presented as the mean ± S.E. Unpaired Student's *t* test and a two-way repeated ANOVA analysis were performed to test for differences between groups. A value of $p < 0.05$ was accepted as statistically significant.

RESULTS

Expression of Recombinant Human S100A1 Protein and Synthesis of S100A1 Peptides—Before studying the effect of S100A1 on contractile performance and SR function, it was important to demonstrate purity and integrity both of recombinantly expressed human S100A1 protein and synthetic S100A1 peptides. Purified S100A1 protein was analyzed by SDS-PAGE and ESI-MS, respectively. Fig. 1*A* depicts a representative silver staining of S100A1 preparations resolved by

4–20% SDS-PAGE. As shown in Fig. 1*A*, purified S100A1 protein consisted of a pure single band migrating as a 10-kDa component without visuable contamination by other proteins. Accurate mass was determined by ESI-MS. The observed peak *m/z* ion values (10416.37 ± 0.35 Da, $n = 5$) correlated well with the calculated mass for human S100A1 protein $C_{465}H_{677}N_{114}S_3O_{153}$ (10,415 Da, Swiss Protein Data Bank number P23297) within the experimental error (0.01%). Specificity of the purified protein was examined by Western blotting. Immunodetection with anti-S100A1 antibody revealed one major band approximately at 10 kDa representing the S100A1 monomer (Fig. 1*B*). In addition, there was a second band of higher molecular mass migrating between 23 and 34 kDa, consistent with dimeric S100A1 aggregates (Fig. 1*B*, *double asterisk*).

Although it has been reported that even application of high concentrations of the Ca^{2+}-binding protein S100A1 protein (~80 μM) to EGTA-buffered Ca^{2+} solutions caused no change in free Ca^{2+} concentration (31), we sought to introduce a synthetic S100A1 peptide model devoid of Ca^{2+}-binding motifs both to exclude any artificial lowering of the free Ca^{2+} concentration by S100A1 protein in our experimental setting and to gain further insight into structure-function relationship of S100A1 effects. Amino acid sequence alignment displayed in Fig. 1*C* compares S100A1 peptides defined by residues 2–16 (*N-terminal* (*N*)), 42–54 (*Hinge-region* (*H*)), and 75–94 (*C-terminal* (*C*)) to the human S100A1 protein primary sequence. The selected peptides encompass nearly 50% of the protein, however, omitting both EF-hand Ca^{2+}-binding domains. Fig. 1*D* exhibits a representative silver staining of the three S100A1 peptides resolved by 4–20% SDS-PAGE, visualizing the high purity that was confirmed by analytical reverse-phase high performance liquid chromatography analysis (data not shown). Molecular weight was determined by the use of matrix-assisted laser desorption ionization-time of flight mass spectroscopy. Peak signals yielded in the mass spectrum (N, 1653.26 ± 0.52 Da; H, 1376.17 ± 0.39 Da; C, 2257.10 ± 0.19; $n = 5$) were nearly identical to the calculated peptide mass (N, 1652 Da; H, 1377 Da; and C, 2258 Da). Immunoprecipitation of endogenous S100A1 protein levels in murine cardiomyocyte, EDL, and Soleus muscle preparations visualized both by silver staining (Fig. 1*E*, *upper panel*) and Western blotting (Fig. 1*E*, *lower panel*) confirmed both differential S100A1 expression levels in murine heart (16.87 ± 1.22 densitometric arbitrary units; 100%), Soleus (6.56 ± 0.89 densitometric arbitrary units; 38% compared with heart), and EDL (0.72 ± 0.04 densitometric arbitrary units; 4.26% compared with heart) as well as S100A1 depletion of striated muscle following saponin treatment. S100A1 monomer and dimer are indicated by *single* and *double asterisks*, respectively.

S100A1 Increases Caffeine-induced SR Ca^{2+} Release and Ca^{2+}-induced Isometric Force Transients in Murine EDL and Soleus Muscle Fibers—S100A1 has been reported to be mainly found in cardiac and slow-twitch skeletal muscle, whereas fast-twitch muscle fibers contain lower amounts of S100A1 protein (6, 32), which could be confirmed by S100A1 immunoprecipitation (Fig. 1*E*). Since S100A1 has been shown to interact with the SR Ca^{2+} release channel/ryanodine receptor (RyR1) reconstituted in lipid bilayers (12), we were interested whether S100A1/RyR1 interaction can modulate SR function and contractile properties of skeletal muscle fibers. To gain direct diffusional access for S100A1 protein and peptides to the myoplasm and its target proteins, the sarcolemma from small EDL and Soleus muscle bundles was rendered permeable by saponin treatment, thus leaving the SR and the contractile apparatus fully intact (24). Importantly, saponin treatment resulted in significant depletion of endogenous S100A1 protein levels both in EDL and Soleus muscle preparations (Fig. 1*E*). According to previous biophysical approaches (12), we first investigated SR Ca^{2+} efflux in response to acute application or preincubation (2 min) both of S100A1 protein and synthetic S100A1 peptides (N/H/C) in our experimental setting. Interestingly, in the presence of 0.5 mM free Mg^{2+} that is believed to inhibit channel opening by occupying the site for calcium activation of the RyR (33) S100A1 interventions failed to directly elicit SR Ca^{2+} release both in Soleus and EDL skeletal muscle preparations.

Therefore, we decided to investigate the impact of S100A1 on activated RyR-mediated SR Ca^{2+} release using caffeine. Caffeine was chosen to initiate RyR1 opening for its ability to increase Ca^{2+} sensitivity of the Ca^{2+} activation site on the SR Ca^{2+} release channel without appreciably affecting channel subconductance and sensitivity to endogenous regulators (*e.g.* ATP) (34, 35), which can be seen in the bell-shaped curve of channel activation *versus* $[Ca^{2+}]$ as a leftward shift of the ascending (activation) arm of the curve with little change in the descending (inhibition) limb (36).

Prior to S100A1 interventions, a series of caffeine-induced control Ca^{2+} releases were established and EDL and Soleus fibers were loaded with Ca^{2+} in such a manner that the peaks of the Ca^{2+}-induced force transients reached ~20–40% of the maximal isometric Ca^{2+}-dependent force. All of the force transients were normalized to maximum force to correct for the rundown of the fiber. Fig. 2 shows typical examples for S100A1 protein (Fig. 2, *A* and *B*) and the S100A1 peptide-(N/H/C) (Fig. 2, *E* and *F*) interventions on isometric force transients in EDL and Soleus muscle fibers compared with control. The addition of S100A1 protein (1 μM) resulted in an equal reversible increase of the isometric force transients both in EDL (+53.7 ± 10.1%, $n = 6$; *, $p < 0.01$) and Soleus (+55.1 ± 4.12%, $n = 5$; *, $p < 0.01$) compared with control (Fig. 2*I*). Application of the S100A1 peptide model (N/H/C) (1 μM) resulted in a similar enhancement in peak amplitudes of the force transients in EDL (+59.9 ± 8.13%, $n = 6$; *, $p < 0.01$) and Soleus (+58.9 ± 9.31%, $n = 7$; *, $p < 0.01$) demonstrating identical activity of the synthetic S100A1 model compared with the native protein (Fig. 2*I*).

Corresponding Ca^{2+} transients for S100A1 protein and S100A1 peptide-(N/H/C) interventions in EDL and Soleus muscle fibers (Fig. 2, *C* and *D* and *G* and *H*) were obtained by transformation of the force transients using the inverse Hill function fitted to the individual pCa-force relationships as previously described (22) that were recorded for every fiber preparation (see "Experimental Procedures") (22, 24, 25). S100A1 protein and peptides (N/H/C) were found to equally enhance calculated peak Ca^{2+} values of the Ca^{2+} transients by +58.7 ± 5.13% ($n = 6$; *, $p < 0.01$) and +52.3 ± 11.3% ($n = 6$; *, $p < 0.01$) in EDL and by +45.9 ± 7.30% ($n = 5$; *, $p < 0.01$) and +48.3 ± 4.17% ($n = 7$; *, $p < 0.01$) in Soleus, respectively, compared with control Ca^{2+} transients (Fig. 2*J*). Moreover, integration of the area (time integral) of the calculated Ca^{2+} transient served as a relative indicator of the amount of Ca^{2+} released from the SR (21, 37). Normalized to the area under the control Ca^{2+} transients, S100A1 interventions (1 μM) significantly enhanced the caffeine-triggered amount of Ca^{2+} released by the SR in EDL (S100A1 protein: +98.0 ± 8.71%, $n = 4$; *, $p < 0.01$; S100A1 peptides (N/H/C): +91.0 ± 9.63%, $n = 4$; *, $p < 0.01$) and Soleus (S100A1 protein: +90.4 ± 12.3%, $n = 5$; *, $p < 0.01$; S100A1 peptides (N/H/C): +87.8 ± 12.4%, $n = 5$; *, $p < 0.01$) muscle fibers compared with control.

Given the equal bioactivity of S100A1 peptides (N/H/C) and S100A1 protein in both skeletal muscle isoforms, the testing of dose dependence was restricted to S100A1 peptides in EDL

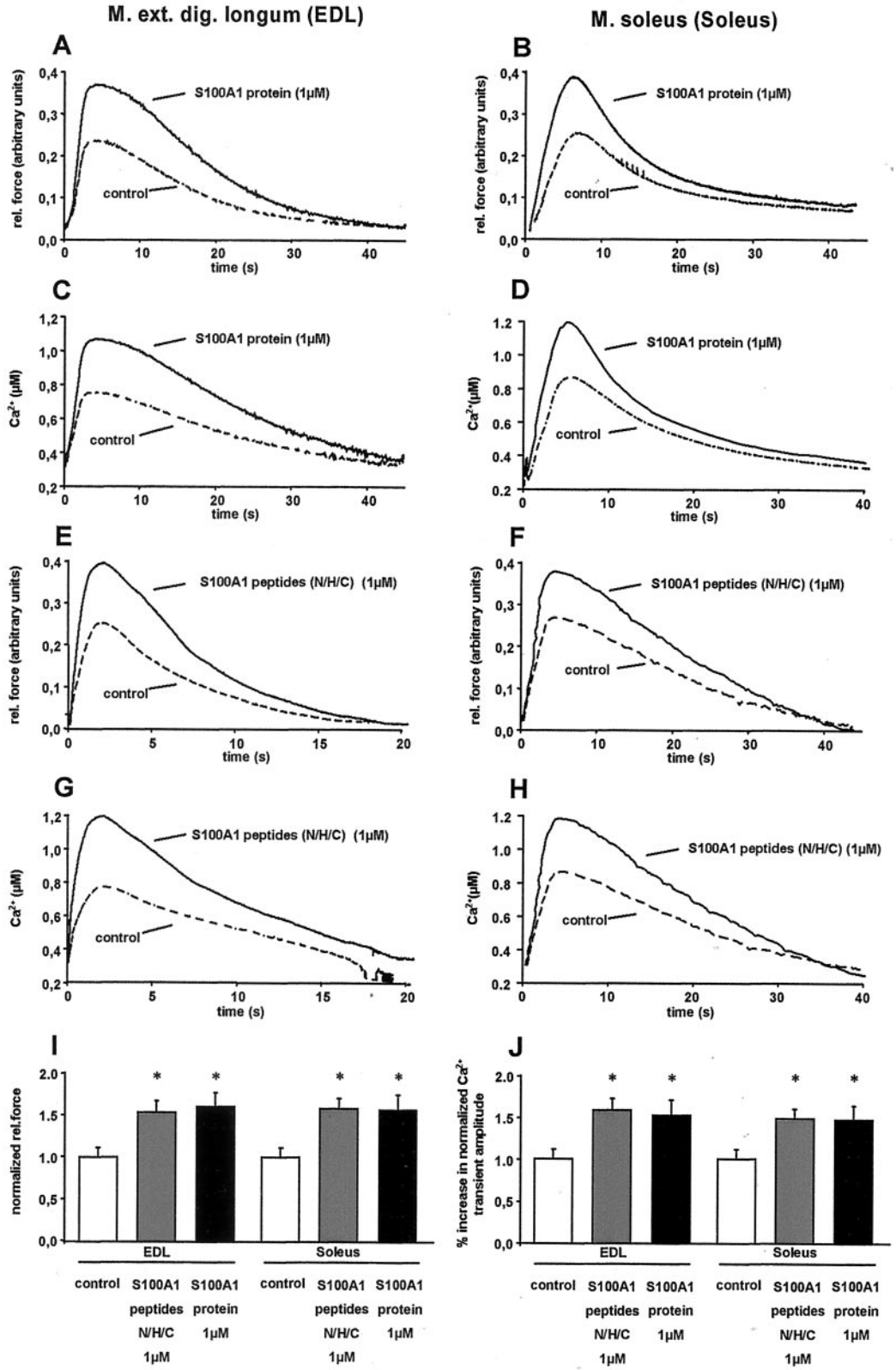

FIG. 2. **S100A1 enhances caffeine-evoked isometric twitch force and Ca^{2+} transients in EDL and Soleus skeletal muscle fibers.** *A–H*, representative superimposed original tracings for S100A1 interventions (S100A1 protein and S100A1 peptides (N/H/C)) in EDL (*left panel*) and Soleus muscle preparations (*right panel*). Isometric force transients are normalized to maximal isometric force, whereas Ca^{2+} transients were obtained as described under "Experimental Procedures." Statistical analysis for the isometric twitch and Ca^{2+}-transient amplitude are given in *I* and *J*, respectively. Values are normalized to the amplitude of control transients. *, $p < 0.01$ compared with control. Data are presented as mean ± S.E.

muscle preparations. Application of incremental concentrations of S100A1 peptides (N/H/C) in a range of 0.001–1 μM revealed a dose-dependent enhancement of caffeine-induced normalized peaks of isometric force and Ca^{2+} transients, respectively (Fig. 3, *A* and *B*). However, increasing concentrations of S100A1 beyond 1 μM resulted again in diminished amplitudes of isometric twitch force and Ca^{2+} transients. With regard to three potential S100A1-binding domains that have

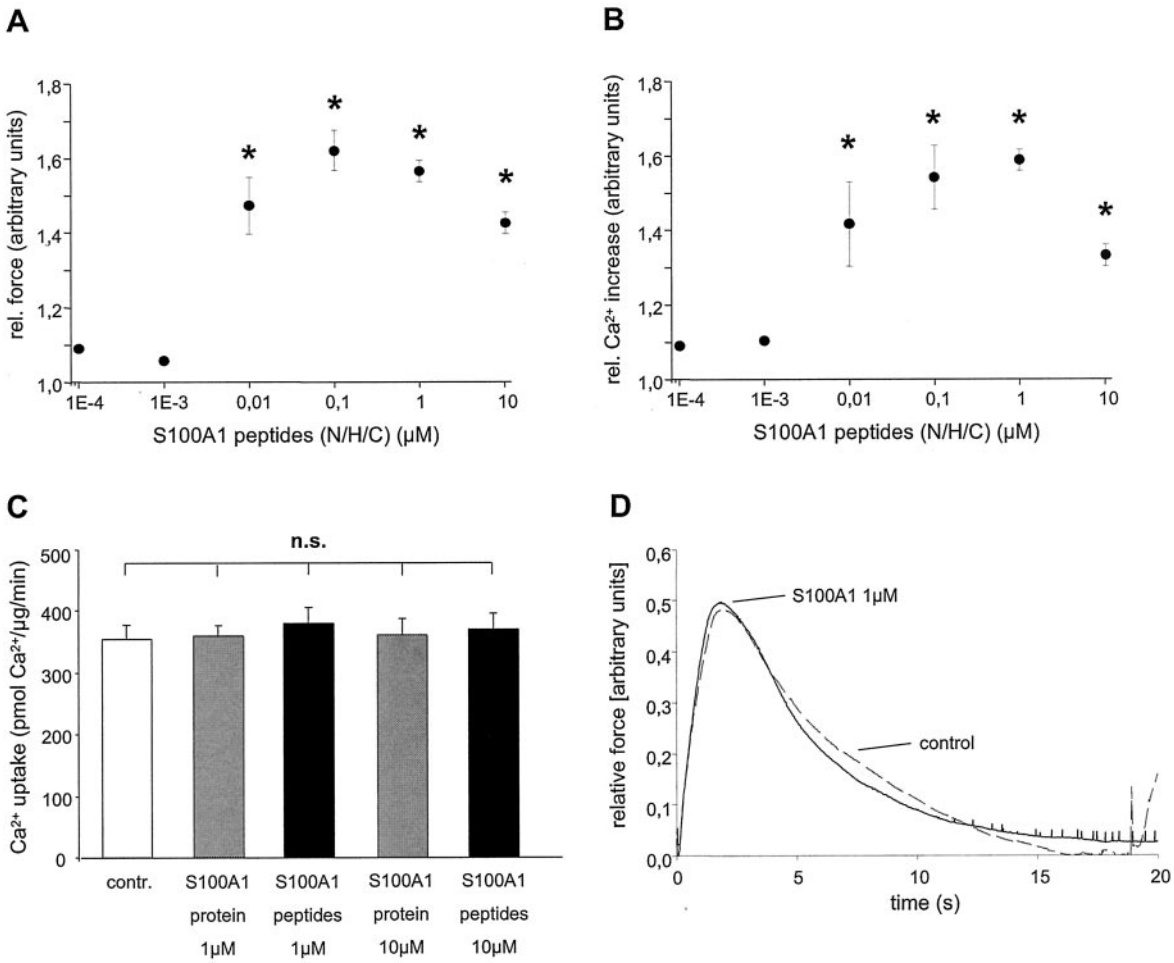

FIG. 3. **S100A1 dose-dependent enhancement of isometric twitch force in skeletal muscle fibers.** Dose-dependent increase of caffeine-induced normalized relative isometric force (*A*) and Ca^{2+}-transient amplitudes by S100A1 in a range of 0.001–1 μM (*B*) are shown. A further rise in S100A1 concentrations (>1 μM) caused a smaller increase of peak force and Ca^{2+} released from the SR. *, $p < 0.05$ compared with control. *C*, unchanged Ca^{2+} uptake rate (pmol Ca^{2+}/μg/min) of EDL SR vesicles in the presence of either S100A1 protein (1 and 10 μM) or S100A1 peptides (N/H/C) (1 and 10 μM) compared with control vesicles. *D*, representative normalized force transients evoked by caffeine application in response to S100A1 peptide-(N/H/C) addition solely to SR-loading solution in skinned EDL muscle fibers. S100A1 (*solid trace*) did not alter SR Ca^{2+} load in skeletal muscle as indicated by the same isometric peak force because of caffeine-induced SR Ca^{2+} release compared with control (*dashed trace*). Similar results were obtained for S100A1 protein (data not shown). Data are presented as mean ± S.E.

been identified on each subunit of the RyR1 (12), these results support the notion of a biphasic Ca^{2+}-dependent action of S100A1 as already described for calmodulin (35, 38).

As S100A1 has been shown to colocalize with the SR in skeletal muscle (6) and inhibition of SERCA activity accounts for increased peak force in skinned fiber preparations (22), the effect both of S100A1 protein and S100A1 peptides on SERCA activity was examined. SERCA activity was assessed by oxalate-facilitated SR Ca^{2+} uptake measurements in SR vesicles from murine EDL. Ca^{2+} uptake was started by the addition of Ca^{2+} to a final concentration >1 μM free [Ca^{2+}], and the decline of the Fura-2 fluorescence within the cuvette was recorded in the presence of 5 mM ruthenium red to inhibit Ca^{2+} release. Following calibration, Ca^{2+} uptake rate (dCa^{2+}/dt; pmol Ca^{2+}/s) for 1 μM free [Ca^{2+}] was calculated from the time constant τ of [Ca^{2+}] decline. Neither the addition of S100A1 protein nor application of peptides (N/H/C) significantly altered SR Ca^{2+} uptake rate compared with control (S100A1 protein: 1 μM, 359 pmol Ca^{2+}/s; S100A1 protein: 10 μM, 367 pmol Ca^{2+}/s; S100A1 peptide: 1 μM, 379 pmol Ca^{2+}/s; S100A1 peptides: 10 μM, 375 pmol Ca^{2+}/s; $n = 6$ for each experiment; p = not significant *versus* control 354 pmol Ca^{2+}/s) (Fig. 3*C*). Moreover, S100A1 impact on SERCA activity and SR Ca^{2+} uptake has also been tested in saponin-skinned muscle fiber preparations. Fig. 3*D* shows that the addition of 1 μM S100A1 peptides to loading solution resulted in unchanged caffeine-induced isometric peak force and corresponding SR Ca^{2+} release, confirming that S100A1 did not alter SR Ca^{2+} loading in our experimental setting. Similar results were obtained for 10 μM S100A1 (data not shown).

S100A1 Domains Differentially Affect SR Function and Contractile Properties of Saponin-skinned Skeletal Muscle Preparations—Because we could show that S100A1 protein enhances caffeine-induced SR Ca^{2+} release in chemically skinned skeletal muscle fibers, we next sought to gain further insight into the structure-function relationship of S100A1/RyR1 interaction. Introduction of the S100A1 peptide-(N/H/C) model enabled us to investigate differential biological effectiveness of distinct S100A1 domains. Fig. 4, *B–D*, displays representative superimposed original tracings of caffeine-induced isometric force transients in EDL muscle preparations in response to S100A1-C, S100A1-H, or S100A1-N peptide interventions compared with control. The addition of the S100A1-C peptide (aa 75–94) resulted in a nearly identical increase in the amplitude of the caffeine-evoked isometric force transient (+51.2 ± 12.1%, $n = 5$; *, $p < 0.01$ *versus* control; #, $p < 0.03$ *versus* S100A1-H peptide) compared with S100A1 protein or the combination of all of the three S100A1 peptides (N/H/C) (Fig. 4*A*).

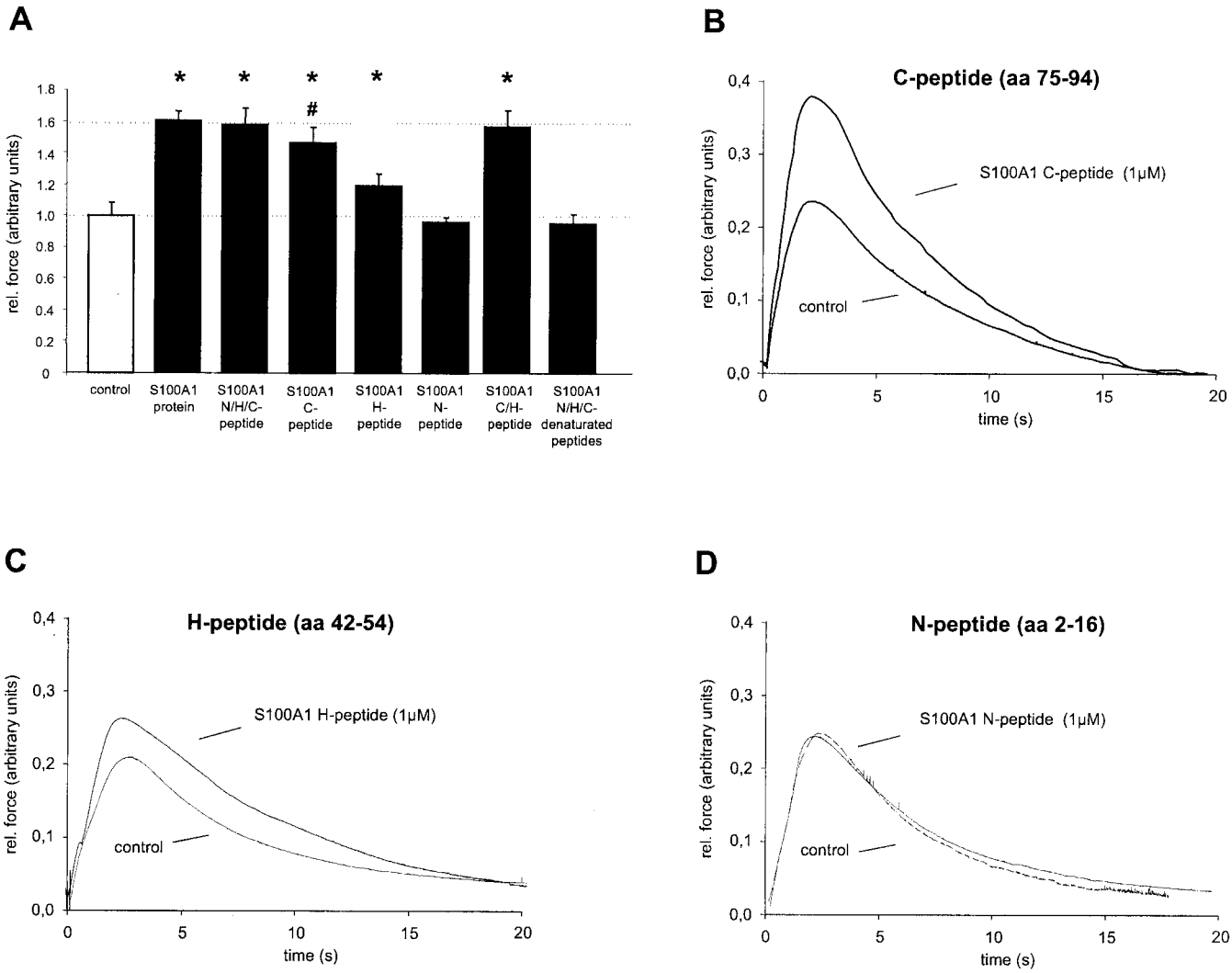

FIG. 4. **Differential increase of isometric twitch force in skeletal muscle fibers by different S100A1 domains.** *A*, differential effects of S100A1 protein and peptides (1 μM) on caffeine-induced normalized isometric twitch force amplitude. *, $p < 0.05$ compared with control; #, $p < 0.05$ compared with S100A1-H peptide. *B–D*, representative superimposed original tracings for the normalized isometric force transient amplitude in response to S100A1 single peptide interventions. Data are presented as mean ± S.E.

Further testing of the single S100A1-H peptide (aa 42–54) revealed a minor but still significant enhancement of the amplitude of the caffeine-evoked isometric force transient (+18.5 ± 8.3%, $n = 5$, *, $p < 0.05$ *versus* control), whereas the addition of the S100A1-N peptide (aa 2–16) displayed no effect (Fig. 4*A*). Additive application both of the S100A1-C and S100A1-H peptide revealed no further increase above the single C-peptide, S100A1 peptides (N/H/C), or the native protein. Importantly, control experiments with degraded "scrambled" S100A1 peptides (N/H/C) that have been subjected to repeated freeze-thaw cycles and intense sonification did not influence the isometric force transient (Fig. 4*A*).

S100A1 Protein and Peptides Does Not Alter Myofilament Ca^{2+} Sensitivity in Murine Fast- and Slow-Twitch Muscle Fibers—S100A1 is assumed to bind to contractile filaments in striated muscle (5) and has been shown to modulate the function of sarcomeric proteins (8, 31, 39). Thus, it was necessary to determine whether S100A1 interventions modulate Ca^{2+} sensitivity of regulatory proteins (*e.g.* troponin C) of the contractile apparatus in skeletal muscle preparations in our experimental approach, which might have contributed to the observed modulation of peak twitch force. The pCa-force relationship was measured both at the beginning and the end of each protocol in EDL and Soleus skinned muscle fibers to determine both Ca^{2+} concentration for half-maximal isometric force activation as a measure of myofilament Ca^{2+} sensitivity (EC_{50} [Ca^{2+}]) and the steepness of the sigmoidal curve (Hill coefficient) as a value for the Ca^{2+}-dependent cooperative interactions among contractile and regulatory proteins. In addition, maximal tension development was recognized as a measure of Ca^{2+}-dependent regulation of strong cross-bridge attachment between the thin and thick filament. In the presence of caffeine application of 1 μM S100A1 protein and S100A1 peptides (N/H/C), neither affected Ca^{2+} sensitivity nor cooperativity in Soleus (S100A1 peptides (N/H/C) (S100A1 peptides, pCa EC_{50} 5.95 ± 0.03, n_{Hill} 2.5 ± 0.18, $n = 4$; S100A1 protein, pCa EC_{50} 5.90 ± 0.02, n_{Hill} 2.35 ± 0.22, $n = 4$; control, pCa EC_{50} 5.86 ± 0.05, n_{Hill} 2.47 ± 0.34, $n = 4$; p = not significant *versus* S100A1) and EDL (S100A1 peptides, pCa EC_{50} 5.31 ± 0.07, n_{Hill} 4.41 ± 0.53, $n = 4$; S100A1 protein, pCa EC_{50} 5.36 ± 0.10, n_{Hill} 4.22 ± 0.21, $n = 4$; control pCa EC_{50} 5.33 ± 0.11, n_{Hill} 4.38 ± 0.31, $n = 4$, p = not significant *versus* S100A1) compared with control in our experimental setting. Accordingly, we found that S100A1 did not alter maximal Ca^{2+}-dependent tension development with regard to normalized maximal tension development of control fibers. In addition, pCa-force relationship for each single S100A1 peptide intervention was also found to be unaltered (data not shown).

DISCUSSION

In striated muscle, RyR is the major channel for Ca^{2+} release from intracellular stores to cause an increase in myoplasmic Ca^{2+} concentration, resulting in muscle contraction. Moreover it is known that the SR Ca^{2+} release channel can interact with a variety of accessory proteins believed to modulate RyR activity (40). In this regard, biophysical approaches have previously been shown that the Ca^{2+}-binding protein S100A1 can interact with the skeletal muscle RyR isoform, resulting in increased open probability of the purified SR Ca^{2+} release channel reconstituted in lipid bilayers (12).

S100A1, a member of the Ca^{2+}-binding protein family known as S100, is the most abundant S100 protein isoform in striated muscle (7, 41) and has been shown to colocalize, in particular, with the sarcoplasmic reticulum and the contractile apparatus (5–7, 32, 42). Although recent studies *in vitro* and *in vivo* have reported on S100A1 to play a crucial role in the regulation of cardiac contractility (8–11), the impact of S100A1 on skeletal muscle contractility remained elusive so far. Therefore, we took advantage of a specific membrane permeabilization with saponin maintaining the cellular architecture of the SR and contractile apparatus and controlling the intracellular milieu (43) to investigate the role of S100A1 in the regulation of SR Ca^{2+} efflux and contractile performance in skeletal muscle fibers.

In this study, we were able to demonstrate for the first time that S100A1/RyR1 interaction results in increased contractile performance both of slow- and fast-twitch skeletal muscle fibers because of enhanced SR Ca^{2+} release. Importantly, despite different endogenous S100A1 protein levels in skeletal muscle isoforms that have been estimated to ~1–10 μM in slow- and 5–20 times less in fast-twitch skeletal muscle (5, 6, 32), reconstitution of chemically S100A1-depleted skeletal muscle fibers with either S100A1 protein or S100A1 peptides (N/H/C) near to their native levels yielded similar effects on isometric force transients and SR Ca^{2+} release. Although slow- and fast-twitch skeletal muscles differ in many ways (*e.g.* metabolism, protein isoform composition, and so forth), they mainly express the same RyR isoform (RyR1), which could partially explain identical effects of S100A1 on SR Ca^{2+} efflux in Soleus and EDL muscle fibers.

However, in our experimental setting S100A1-mediated enhancement of SR Ca^{2+} release only occurred with caffeine while in its absence S100A1 interventions failed to activate RyR1 opening. Thus, at first glance our data appears to disagree with Treves *et al.* (12) who previously reported on S100A1 protein to directly increase open probability of the purified RyR1 reconstituted in lipid bilayers. One important reason for this apparent discrepancy may be that these experiments were carried out in the absence of Mg^{2+} (12), whereas in contrast, S100A1 effects on SR Ca^{2+} release in saponin-skinned skeletal muscle preparations were studied in the presence of Mg^{2+} near its native concentrations. This is essential to note because Mg^{2+} is as a central inhibitor of Ca^{2+}-dependent activation of the release channel and its physiological concentration near 1 mM is necessary in maintaining the RyR1 channels closed at rest (33, 44, 45). S100A1 effects on single channel-gating properties therefore occurred under experimental conditions when the channel was strongly sensitized to Ca^{2+}-dependent activation. Because the mechanism of caffeine is also based on increased channel sensitivity to activation by Ca^{2+} (35, 36, 46) both studies consistently show that S100A1 protein principally enhances RyR1 opening under conditions that sensitize the channel to Ca^{2+} (absence of Mg^{2+}, caffeine).

Taken together, S100A1 appears to directly activate RyR1 opening in the absence of Mg^{2+} while physiological levels of Mg^{2+} effectively prevent this effect. Therefore, we propose that under physiological conditions that the L-type Ca^{2+} channel voltage-gated control mechanism and the presence of Mg^{2+} provide the intrinsic mechanisms to avoid spontaneous and/or sustained RyR1 opening via S100A1. However, once RyR1 activation is promoted, *e.g.* by drug- or voltage-induced opening of the channel, we speculate that S100A1 protein enhances activated SR Ca^{2+} release by increasing the channel open probability. In addition, it seems noteworthy that dose-dependent S100A1-mediated amplification of SR Ca^{2+} release in our experimental setting first occurred at nanomolar S100A1 concentrations similar to effective S100A1 concentrations reported by Treves *et al.* (12). This finding strongly supports the notion that even low native S100A1 protein levels as found in EDL muscle are already sufficient to regulate SR function and contractile performance. Thus, taking advantage of a more physiological approach, we speculate that S100A1 might rather serve as an endogenous enhancer of SR Ca^{2+} release in skeletal muscle than to directly open the SR Ca^{2+} release channel.

Based on primary sequence alignment (47) and three-dimensional reconstruction of S100A1 protein explored by NMR spectroscopy (14), we next applied a synthetic S100A1 peptide model to gain further insight into structure-function relationship of S100A1/RyR1 interaction. Importantly, as described above application for all of the three S100A1 peptides (N/H/C), omitting both Ca^{2+}-binding loops revealed similar effects in slow- and fast-twitch skeletal muscle preparations compared with the native protein. Testing of single S100A1 peptides revealed that at least the S100A1 C-terminal amino acid sequence 75–94 exerts nearly an identical biological activity as the native protein. Moreover, the S100A1 hinge region encompassing the amino acid sequence 42–54 also displayed biological activity albeit less than the S100A1 C terminus, whereas the N-terminal extension displayed no effect on SR Ca^{2+} release.

Thus, our data support previous assumptions that both the C-terminal residue and the hinge region, which are buried in the apoform (48) and exposed in the calcium-bound form (49), mediate selectivity in S100 protein target binding and biological activity while the N-terminal extension is recognized to stabilize the dimeric structure of S100 proteins (50). In addition, we were able to show that different S100A1 domains exert differential biological activity because the C-terminal extension was found to be ~2–3 times more effective than the linker region. These findings seem to be specific for S100A1 interventions as the characterization of protein and peptide preparations revealed highest purity and integrity of the compounds, whereas denatured S100A1 peptides did not yield any biological effect.

Because myofilament Ca^{2+} sensitivity is another important factor that essentially contributes to the regulation of contractile force in skeletal muscle (43), we analyzed the impact of S100A1 interventions on the pCa-force relationship. Although an altered Ca^{2+} affinity of myofilament-associated regulator proteins by S100A1 could have contributed to the observed increase in peak force, S100A1 neither influenced Ca^{2+} sensitivity nor cooperativity of the contractile apparatus in our experimental setting. Further, Adhikari and Wang (31) showed that S100A1 protein can decrease myofilament Ca^{2+} sensitivity of skinned rabbit psoas skeletal muscle fibers. However, it should be noted that the study by Adhikari and Wang (31) was carried out at a shorter sarcomere length (2.1–2.2 μm) and that there are major differences with respect to muscle-specific and species-specific fiber-type composition (51–53) to explain the different findings of S100A1 effects on pCa-force relationship.

Because previous studies reported a possible interaction of S100A1 with the skeletal muscle SR Ca^{2+}-ATPase isoform (6),

we sought to investigate whether S100A1 might affect SR Ca^{2+} uptake in skeletal muscle by the use of fluorescence-based Ca^{2+} uptake measurements in purified SR vesicles. Consistent with reports by Fano *et al.* (54), neither S100A1 protein nor S100A1 peptides (N/H/C) were found to alter SR Ca^{2+} uptake rate in our assay system. Because purification of SR vesicles may somewhat alter the responsiveness to endogenous regulators because of the loss of membrane compounds, we additionally assessed the effect of S100A1 on SR Ca^{2+} loading in saponin-skinned fiber preparations. In accordance with our fluorescence-based measurements, SR Ca^{2+} load as determined by caffeine-induced contractures was similar for S100A1 interventions and controls in skeletal muscle fibers. Thus, in skeletal muscle, S100A1 does not appear to indirectly modulate Ca^{2+}-activated force by changing the rate of SR Ca^{2+} uptake.

In conclusion, we have shown the ability of S100A1/RyR1 interaction to enhance Ca^{2+} efflux from the intact SR in saponin-skinned skeletal muscle fibers resulting in increased contractile performance. Introducing a novel synthetic S100A1 peptide model allowed us to identify specific S100A1 domains that are critically implicated in the structure-function relationship of S100A1/RyR1 interaction. Interestingly, despite higher endogenous S100A1 protein levels in slow- than in fast-twitch skeletal muscle, both skeletal muscle isoforms exerted identical responsiveness to S100A1 interventions. Given that S100A1 has recently been proven to play a central role in the regulation of myocardial contractile performance (8–11), we propose an important physiological role for S100A1 in skeletal muscle *in vivo* to serve as an endogenous enhancer of activated RyR1-mediated sarcoplasmic Ca^{2+} release, thereby enhancing skeletal muscle contractile performance. However, further experiments taking advantage of *in vivo* genetic manipulation of endogenous S100A1 protein levels in skeletal muscle will have to finally address this issue.

Acknowledgment—We are indebted to Dr. John Solaro for helpful and critical discussion of the paper.

REFERENCES

1. Remppis, A., Greten, T., Schafer, B. W., Hunziker, P., Erne, P., Katus, H. A., and Heizmann, C. W. (1996) *Biochim. Biophys. Acta* **1313,** 253–257
2. Ehlermann, P., Remppis, A., Guddat, O., Weimann, J., Schnabel, P. A., Motsch, J., Heizmann, C. W., and Katus, H. A. (2000) *Biochim. Biophys. Acta* **1500,** 249–255
3. Polyakov, A. A., Huber, P. A., Marston, S. B., and Gusev, N. B. (1998) *FEBS Lett.* **422,** 235–239
4. Donato, R. (2001) *Int. J. Biochem. Cell Biol.* **33,** 637–668
5. Maco, B., Brezova, A., Schafer, B. W., Uhrik, B., and Heizmann, C. W. (1997) *Gen. Physiol. Biophys.* **16,** 373–377
6. Zimmer, D. B. (1991) *Cell Motil. Cytoskeleton* **20,** 325–337
7. Kato, K., and Kimura, S. (1985) *Biochim. Biophys. Acta* **842,** 146–150
8. Most, P., Bernotat, J., Ehlermann, P., Pleger, S. T., Reppel, M., Borries, M., Niroomand, F., Pieske, B., Janssen, P. M., Eschenhagen, T., Karczewski, P., Smith, G. L., Koch, W. J., Katus, H. A., and Remppis, A. (2001) *Proc. Natl. Acad. Sci. U. S. A.* **98,** 13889–13894
9. Most, P., Remppis, A., Pleger, S. T., Löffler, E., Ehlermann, P., Berustat, J., Kleuss, C., Heierhorst, J., Ruiz, P., Witt, H., Karczewski, P., Mao, L., Rockman, H. A., Duncan, S. J., Katus, H. A., and Koch, W. J. (2003) *J. Biol. Chem.*, in press
10. Remppis, A., Most, P., Löffler, E., Ehlermann, P., Bernotat, J., Pleger, S. T., Börries, M., Repper, M., Fischer, J., Koch, W. J., Smith, G. L., and Katus, H. A. (2002) *Basic Res. Cardiol.* **97,** I56–I62
11. Du, X. J., Cole, T. J., Tenis, N., Gao, X. M., Kontgen, F., Kemp, B. E., and Heierhorst, J. (2002) *Mol. Cell. Biol.* **22,** 2821–2829
12. Treves, S., Scutari, E., Robert, M., Groh, S., Ottolia, M., Prestipino, G., Ronjat, M., and Zorzato, F. (1997) *Biochemistry* **36,** 11496–11503
13. Endo, M., and Iino, M. (1980) *J. Muscle Res. Cell Motil.* **1,** 89–100
14. Wang, Z., Zhang, H., Ding, Y., Wang, G., Wang, X., Ye, S., Bartlam, M., Tang, H., Liu, Y., Jiang, F., Barraclough, R., Rudland, P. S., and Rao, Z. (2001) *Acta Crystallogr. D Biol. Crystallogr.* **57,** 882–883
15. Baudier, J., and Gerard, D. (1986) *J. Biol. Chem.* **261,** 8204–8212
16. Baudier, J., Glasser, N., and Gerard, D. (1986) *J. Biol. Chem.* **261,** 8192–8203
17. Ehlermann, P., Remppis, A., Most, P., Bernotat, J., Heizmann, C. W., and Katus, H. A. (2000) *J. Chromatogr.* **737,** 39–45
18. Engelkamp, D., Schafer, B. W., Erne, P., and Heizmann, C. W. (1992) *Biochemistry* **31,** 10258–10264
19. Miranda, L. P., Tao, T., Jones, A., Chernushevich, I., Standing, K. G., Geczy, C. L., and Alewood, P. F. (2001) *FEBS Lett.* **488,** 85–90
20. Oakley, B. R., Kirsch, D. R., and Morris, N. R. (1980) *Anal. Biochem.* **105,** 361–363
21. Fink, R. H., and Stephenson, D. G. (1987) *Pflugers Arch. Eur. J. Physiol.* **409,** 374–380
22. Makabe, M., Werner, O., and Fink, R. H. (1996) *Pflugers Arch. Eur. J. Physiol.* **432,** 717–726
23. Fink, R. H., Stephenson, D. G., and Williams, D. A. (1990) *J. Physiol.* (*Lond.*) **420,** 337–353
24. Uttenweiler, D., Weber, C., and Fink, R. H. (1998) *Biophys. J.* **74,** 1640–1653
25. Kunst, G., Stucke, A. G., Graf, B. M., Martin, E., and Fink, R. H. (2000) *Anesthesiology* **93,** 832–836
26. Chu, A., Dixon, M. C., Saito, A., Seiler, S., and Fleischer, S. (1988) *Methods Enzymol.* **157,** 36–46
27. Smith, G. L., Duncan, A. M., Neary, P., Bruce, L., and Burton, F. L. (2000) *Am. J. Physiol.* **279,** H577–H585
28. Grynkiewicz, G., Poenie, M., and Tsien, R. Y. (1985) *J. Biol. Chem.* **260,** 3440–3450
29. Fabiato, A., and Fabiato, F. (1979) *J. Physiol.* (*Lond.*) **75,** 463–505
30. Ehlermann, P., Redweik, U., Blau, N., Heizmann, C. W., Katus, H. A., and Remppis, A. (2001) *Gen. Physiol. Biophys.* **20,** 203–207
31. Adhikari, B. B., and Wang, K. (2001) *FEBS Lett.* **497,** 95–98
32. Haimoto, H., and Kato, K. (1987) *J. Neurochem.* **48,** 917–923
33. Lacampagne, A., Klein, M. G., and Schneider, M. F. (1998) *J. Gen. Physiol.* **111,** 207–224
34. Lamb, G. D., Cellini, M. A., and Stephenson, D. G. (2001) *J. Physiol.* (*Lond.*) **531,** 715–728
35. Meissner, G. (1994) *Annu. Rev. Physiol.* **56,** 485–508
36. Meissner, G., Rios, E., Tripathy, A., and Pasek, D. A. (1997) *J. Biol. Chem.* **272,** 1628–1638
37. Lamb, G. D., and Cellini, M. A. (1999) *J. Physiol.* (*Lond.*) **519,** 815–827
38. Tripathy, A., Xu, L., Mann, G., and Meissner, G. (1995) *Biophys. J.* **69,** 106–119
39. Yamasaki, R., Berri, M., Wu, Y., Trombitas, K., McNabb, M., Kellermayer, M. S., Witt, C., Labeit, D., Labeit, S., Greaser, M., and Granzier, H. (2001) *Biophys. J.* **81,** 2297–2313
40. Franzini-Armstrong, C., and Protasi, F. (1997) *Physiol. Rev.* **77,** 699–729
41. Zimmer, D. B., Song, W., and Zimmer, W. E. (1991) *Brain Res. Bull.* **27,** 157–162
42. Kato, K., Kimura, S., Haimoto, H., and Suzuki, F. (1986) *J. Neurochem.* **46,** 1555–1560
43. Gordon, A. M., Homsher, E., and Regnier, M. (2000) *Physiol. Rev.* **80,** 853–924
44. Gonzalez, A., Kirsch, W. G., Shirokova, N., Pizarro, G., Stern, M. D., and Rios, E. (2000) *J. Gen. Physiol.* **115,** 139–158
45. Lamb, G. D., and Stephenson, D. G. (1991) *J. Physiol. (Lond.)* **434,** 507–528
46. Herrmann-Frank, A., Luttgau, H. C., and Stephenson, D. G. (1999) *J. Muscle Res. Cell Motil.* **20,** 223–237
47. Heizmann, C. W., and Cox, J. A. (1998) *Biometals* **11,** 383–397
48. Drohat, A. C., Amburgey, J. C., Abildgaard, F., Starich, M. R., Baldisseri, D., and Weber, D. J. (1996) *Biochemistry* **35,** 11577–11588
49. Smith, S. P., Barber, K. R., Dunn, S. D., and Shaw, G. S. (1996) *Biochemistry* **35,** 8805–8814
50. Groves, P., Finn, B. E., Kuznicki, J., and Forsen, S. (1998) *FEBS Lett.* **421,** 175–179
51. Wang, L. C., and Kernell, D. (2001) *J. Anat.* **199,** 631–643
52. Hamalainen, N., and Pette, D. (1993) *J. Histochem. Cytochem.* **41,** 733–743
53. Aigner, S., Gohlsch, B., Hamalainen, N., Staron, R. S., Uber, A., Wehrle, U., and Pette, D. (1993) *Eur. J. Biochem.* **211,** 367–372
54. Fano, G., Marsili, V., Angelella, P., Aisa, M. C., Giambanco, I., and Donato, R. (1989) *FEBS Lett.* **255,** 381–384